RESEARCH ARTICLE

The roots of the drought: Hydrology and water uptake strategies mediate forest-wide demographic response to precipitation

Rutuja Chitra-Tarak[1,2,3] | Laurent Ruiz[2,4,5] | Handanakere S. Dattaraja[1] | M. S. Mohan Kumar[2] | Jean Riotte[2,4] | Hebbalalu S. Suresh[1] | Sean M. McMahon[3] | Raman Sukumar[1,6]

[1]Centre for Ecological Sciences, Indian Institute of Science, Bangalore, India; [2]Indo-French Cell for Water Sciences, IISc-IRD Joint Laboratory, Indian Institute of Science, Bangalore, India; [3]Smithsonian Institution Forest Global Earth Observatory, Smithsonian Environmental Research Center, Edgewater, MD, USA; [4]IRD, UMR 5563 GET, Université de Toulouse, CNRS, Toulouse, France; [5]UMR SAS, INRA, Agrocampus Ouest, Rennes, France and [6]Divecha Centre for Climate Change, Indian Institute of Science, Bangalore, India

Correspondence
Rutuja Chitra-Tarak
Email: chitra-tarakr@si.edu
Laurent Ruiz
Email: laurent.ruiz@inra.fr
Raman Sukumar
Email: rsuku@iisc.ac.in

Present address
Rutuja Chitra-Tarak, Smithsonian Institution Forest Global Earth Observatory (Forest-GEO), Smithsonian Environmental Research Center, Edgewater, MD 21037, USA

Abstract

1. Drought-induced tree mortality is expected to increase globally due to climate change, with profound implications for forest composition, function and global climate feedbacks. How drought is experienced by different species is thought to depend fundamentally on where they access water vertically below-ground, but this remains untracked so far due to the difficulty of measuring water availability at depths at which plants access water (few to several tens of metres), the broad temporal scales at which droughts at those depths unfold (seasonal to decadal), and the difficulty in linking these patterns to forest-wide species-specific demographic responses.

2. We address this problem through a new eco-hydrological framework: we used a hydrological model to estimate below-ground water availability by depth over a period of two decades that included a multi-year drought. Given this water availability scenario and 20 year long-records of species-specific growth patterns, we inversely estimated the relative depths at which 12 common species in the forest accessed water via a model of water stress. Finally, we tested whether our estimates of species relative uptake depths predicted mortality in the multi-year drought.

3. The hydrological model revealed clear below-ground niches as precipitation was decoupled from water availability by depth at multi-annual scale. Species partitioned the hydrological niche by diverging in their uptake depths and so in the same forest stand, different species experienced very different drought patterns, resulting in clear differences in species-specific growth. Finally, species relative water uptake depths predicted species mortality patterns after the multi-year drought. Species that our method ranked as relying on deeper water were the ones that had suffered from greater mortality, as the zone from which they access water took longer to recharge after depletion.

4. *Synthesis*. This research changes our understanding of how hydrological niches operate for trees, with a trade-off between realized growth potential and survival under drought with decadal scale return time. The eco-hydrological framework highlights the importance of species-specific below-ground strategies in predicting forest response to drought. Applying this framework more broadly may help us better understand species coexistence in diverse forest communities and improve mechanistic predictions of forests productivity and compositional change under future climate.

KEYWORDS

climate change, decoupling, drought, evolutionary strategies, hydrological niche segregation, mortality, rooting depth, seasonally dry tropical forest, temporal niche

1 | INTRODUCTION

Improving predictions of future forest structure and function is essential to global estimates of atmospheric carbon, climate systems and biodiversity. Drought-induced tree mortality is now thought to be a major threat to temperate and tropical forests (Allen, Breshears, & McDowell, 2015; Allen et al., 2010) and much of the concern for forest response to climate centres around tree species' response to drought (Anderegg, Kane, & Anderegg, 2013; Choat et al., 2012; McDowell et al., 2008). Tree growth or the primary productivity of forests is also highly water-dependent, and can indicate the forests' functional response to water stress. Dynamic Global Vegetation Models generally cannot predict drought-induced mortality accurately because many critical processes that lead from meteorological drought to death are unknown or poorly understood (Allen et al., 2015; Anderegg, Anderegg, & Berry, 2013; McDowell et al., 2008; Meir, Mencuccini, & Dewar, 2015). Model projections of net primary productivity are also fundamentally linked to predicted water resources, and uncertainty in these links have led to highly varied predictions of atmospheric and terrestrial carbon stock in model projections (Cramer et al., 2001; Friend et al., 2014; Ichii et al., 2007).

Especially lacking in our understanding of mortality and productivity response to precipitation dynamics are estimates of plant-available water vertically below-ground on temporal scales at which droughts unfold (Schwinning, 2010). Water uptake, which is determined by species-specific hydraulic traits and root depth, further determines the drought actually experienced by trees. Quantifying both species-specific water uptake depth as well as where in the vertical soil profile a "drought" exists is challenging. This is due to the difficulty in knowing comprehensively across the forest where an individual's roots are, from which depth roots are actively taking water, and at which depths the water is available.

Multiple spatio-temporal niches by rooting depth may evolve due to the stochastic nature of precipitation events combined with complex temporal patterns of water movement through the vadose zone (Schwinning, 2010; Schwinning & Kelly, 2013)—the unsaturated zone made up of soil and weathered rock above the groundwater table. However, most studies exploring drought impacts propose access to water based on precipitation and surface soil moisture patterns, ignoring the complex, but critical, dynamics of below-ground water movement, rooting depth and uptake strategies (Rodriguez-Iturbe, 2000; Rodriguez-Iturbe, Porporato, Laio, & Ridolfi, 2001).

No current methodological approach includes water uptake depth dynamics for multiple tree species in a diverse forest, at temporal scales over which droughts unfold and depths at which trees experience drought. One reason for this is that rooting depths for adult trees are not only extremely difficult to obtain, but would not necessarily reveal realized species-specific dynamics of water uptake depths. Tracer studies that infer uptake depths from natural isotopic gradients are typically limited to soil depths of about 1 m or to special cases where water use from soil vs. groundwater is differentiated. Injected tracer experiments are limited in space, time and species diversity. Few recent studies demonstrate the importance of hydrological niche separation to explain species coexistence based on below-ground observations (Silvertown, Araya, & Gowing, 2015). However, due to methodological constraints, they too are limited to few species (typically 2) and focus on niches operating at very shallow depths (about 1 m) or on contrasts between species using vadose zone vs. groundwater.

We provide a new analytical framework to test the spatial and long-term temporal dynamics of below-ground water acquisition and inference on tree community dynamics. This framework models first the vertical and temporal dynamics of water, second, the relative depths at which species access this water based on observed growth patterns, and third, the potential penalties of these access strategies based on species' mortality patterns. Specifically, we test the following hypotheses: (1) Water availability is decoupled from precipitation events by depth, creating a vertically heterogeneous water environment at any given time; (2) relative water availability at these different depths can translate into consistent growth patterns of different species over time depending on species hydraulic/water uptake parameters; (3) common species will show distinct water uptake depths (partition the hydrological niche both in space and time); and (4) species water uptake strategies will result in differential mortality response to extreme droughts.

2 | MATERIALS AND METHODS

2.1 | Demographic data

We derived growth and mortality from permanent forest plot censuses from the 50 ha Mudumalai Forest Dynamics Plot (MFDP) (11°35′N,

76°32′E, 910–1,030 m a.s.l.) in Mudumalai National Park, a seasonally dry tropical forest situated in the rain shadow of the Western Ghats biodiversity hotspot in India. At the MFDP, every woody stem above 1 cm DBH has been tagged with a unique number, identified to species or morpho-species level and mapped (Condit, Lao, Singh, Esufali, & Dolins, 2014; Sukumar et al., 1992). Every 4 years, from 1988 to 2012, each woody stem was re-measured. Mortality and recruitment (stems entering the ≥10 mm DBH class) were recorded every year from 1989 to 2008 and cause of mortality was recorded as either fire, herbivory by large mammal such as elephants or "other causes" (Chitra-Tarak et al., 2017).

For growth data, we selected from the MFDP the set of single-stemmed trees (above 10 mm DBH) that had DBH data available throughout the study period from 1992 to 2012. Individual tree growth rate (cm/year) was calculated as the difference between DBH measured in successive censuses, divided by the inter-census interval. We removed from analyses those trees (n = 110) with "spike" growth rates—those greater than two standard deviations from the mean growth rate of a tree over all census intervals. Given the distribution of growth rates (mean [5%, 95% quantiles]; 0.2 [0.05, 0.6] cm/year), we considered rates beyond (−0.5, 1.5) cm/year in any given census as erroneous and removed those trees (n = 361) from the analysis. Finally, we retained species with sample size greater than 35 trees for further analyses (7,677 trees belonging to 12 species). These 12 species represented two-thirds of the trees in the plot, with four co-dominant species representing half of the trees (Appendix S1.1). Since growth rate change with tree size, we calculated time series of growth rates within narrow size classes. Quantile-based size classes were constructed within species—five each for the four co-dominant species and three each for the rest. Time series of median growth rates (Observed growth$_{4-yearly}$) for each size class by species were used for further analyses (n = 11–441 per size class depending on species; Figure S1) (Chitra-Tarak et al., 2017). We did not expect significant size/age effect on growth within each size class, since most trees remained in the same size class over 20 years due to slow growth rates.

2.2 | Hydrological data

The Mulehole (pronounced as Mʊlehʊle) catchment (11°44′N, 76°27′E, 820–910 m a.s.l.; Braun et al., 2009; Descloitres et al., 2008; Riotte et al., 2014; Ruiz et al., 2010) in Bandipur National Park is about 25-km north-west of the MFDP in a similar geological, climatic and vegetation context (Pulla, Riotte, Suresh, Dattaraja, & Sukumar, 2016). In Mulehole, observations of stream discharge and water-table levels are available from 2003 to 2013 and daily rainfall time series from 1970 to 2013. Hourly temperature, relative humidity, global radiation and wind speed data allowed the calculation of Penman's evapotranspiration (Allen, Pereira, Raes, & Smith, 1998). Annual rainfall at Mulehole is 1,095 ± 236 mm (M ± SD for 1988–2013) and annual PET is 980 ± 64 mm (M ± SD for 2004–2010). Since weather data to calculate PET were not available throughout the study period, we recycled daily PET of 2004 for all years. Daily rainfall data for MFDP were available from Kargudi (1990–2013), the nearest rain gauge station (located

4 km away) with M ± SD annual precipitation of 1,245 ± 278 mm, 70% of which is received during the summer monsoon (June to September; Chitra-Tarak et al., 2017; Dattaraja et al., 2013).

Soils in this region, classified as Alfisols and Mollisols, are rich in clay (sandy clay loam and sandy clay) and are developed over immature (still rich in primary minerals) saprolite (weathered rock; Pulla et al., 2016). See Appendix S1.6 for estimates of Available Water Holding Capacities of these substrates. While soils run 1–2 m deep, total thickness of the vadose zone is estimated at 7–35 m based on local geophysical studies (Braun et al., 2009; Ruiz et al., 2010).

2.3 | Eco-hydrological modelling framework

The modelling framework was developed in three steps. Details of the models are given in the following sections.

1. First, the daily water availability by depth in the soil, as well as in the shallow and deep weathered rock zones above the water-table, was simulated with the Soil–Vegetation–Atmosphere (SVAT) model COMFORT (Ruiz et al., 2010).
2. Second, a daily water-stress index was calculated for each species-size class as the ratio between water supply (a function of water availability provided by COMFORT and species-size class-specific hydraulic parameters) and demand (a function of potential evapotranspiration and leaf area index [LAI]).
3. Finally, hydraulic parameters were calibrated for each species-size class using the Generalized likelihood uncertainty estimation (GLUE) methodology (see below), which maximizes correlation between time series of cumulated water-stress index and growth.

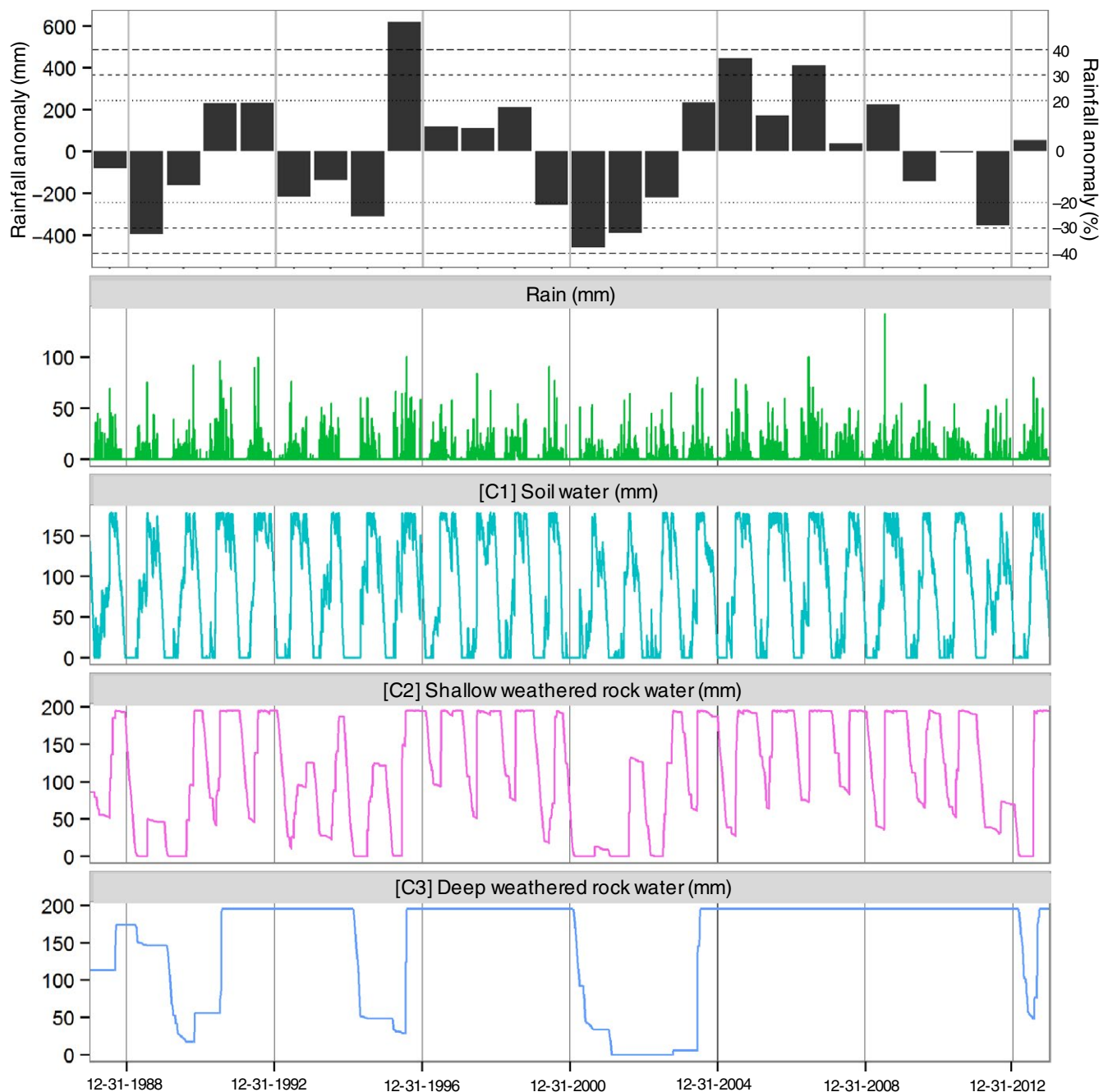### 2.3.1 | Hydrological model COMFORT

Below-ground water availability in the vadose zone was simulated using the hydrological model COMFORT (Ruiz et al., 2010)—a dynamic water balance model for forested catchments, calibrated and validated at the Mulehole watershed. This model balances the observed incoming rainfall against interception, stream discharge, evaporation from the soil, transpiration of water from vegetation (as a big leaf model) from soil and weathered rock zones, recharge of these zones, and recharge of the water-table. This model assumes that trees use water from the vadose zone (unsaturated zone from the top soil to the groundwater table) and not from the groundwater (ability specific to phreatophytes).

COMFORT in effect is a low-pass filter that converts observed high frequency variation in the rainfall pattern into the observed low frequency variation in groundwater levels by redistributing—in vertical space and time—this signal dampening.

To allow for finer resolution of variation in water availability by depth, we used three vadose zone compartments, one soil [C_1] and two equal sized weathered rock zones [C_2, C_3], instead of one soil and one weathered rock zone used in Ruiz et al. (2010). Parameter values, however, remained similar after re-calibrating the model

with longer dataset of stream discharge and water-table levels (2003–2013 compared to earlier 2003–2007). The model accurately simulated observed variations in groundwater level, which was always deeper than 30 m throughout the simulation period (depth of the vadose zone ≥30 m). The calibrated maximum Available Water Content (AWC, or the plant available water) was M_{1max} = 179.2 mm and M_{2max} = M_{3max} = 195.6 mm. The model was run for the MFDP to obtain an estimate of daily water availability for each compartment using local rainfall data (1989–2013) (Figure 1). Although we used

Mulehole rainfall data (1979–1989) for initializing this run, to avoid initialization inaccuracies, model outputs of water availability at MFDP were used only from 1992 onwards. We used the same model parameters as in Mulehole, as vegetation, climate, soils and bedrock are similar (Pulla et al., 2016). Nevertheless, we tested the modelling framework using a range of AWC for the weathered rock zone from 200 to 500 mm, and found that the ranking of species uptake depth, as estimated from model inversion below, was not significantly sensitive to this (results not shown). Our chosen study period from

FIGURE 1 Below-ground water availability as estimated by the hydrological model COMFORT at MFDP, Mudumalai National Park, southern India. 1988 to 2013 time series—from top to bottom—of annual rainfall anomaly, observed daily rainfall, and simulated water content of three below-ground compartments. Grey vertical lines are the year-ends approximately marking the completion of Mudumalai 4-yearly growth censuses [Colour figure can be viewed at wileyonlinelibrary.com]

1992 to 2012 included one prolonged meteorological drought, with rainfall anomalies in the range of −20% to −40% successively over 4 years from 2000 to 2003, besides a few shorter and/or less intense meteorological droughts (Figure 1, Figure S2).

2.3.2 | Water-stress model

Having determined community-level water availability by depth and in time, we developed a novel conceptual model to calculate a daily water-stress coefficient (water supply-to-demand ratio) for each species-size class combination. For each species-size class, this model represents water uptake in a phenomenological way (known as "macroscopic method" in the field of hydrology) by integrating root access and other hydraulic properties over each compartment of the vadose zone, that is unlike approaches that explicitly model root physiology and physics (see e.g. Couvreur, Vanderborght, & Javaux, 2012 for a discussion on respective advantages of both approaches, and Appendix S1.2).

We modelled water supply to be a function of daily plant available water in each below-ground compartment as simulated by the model COMFORT at MFDP ($M_1(t)$, $M_2(t)$ and $M_3(t)$; Figure 1), and access of this water determined by six phenomenological hydraulic parameters specific to each species-size class. That is, for each species-size class, two parameters were estimated for each compartment—one representing "normalized root density" (R) and the other (δ) determining the shape of the hydraulic restriction curve. For interpretation of parameter R (range 0–1, dimensionless), see Appendix S1.3. Parameter δ may relate to both above- and/or below-ground hydraulic properties that regulate water uptake under water depletion (for example, properties driving conductivity loss under negative water potential or stomatal strategy).

For each species-size class, we modelled hydraulic restriction ($HR_i(t)$) in each compartment i as follows:

$$HR_i(t) = \left(\frac{M_i(t)}{M_{i\,max}} \right)^{\delta_i},$$

where $M_i(t)$ and $M_{i\,max}$ are the actual and maximum AWC of compartment C_i, respectively, and δ_i (range 0–2, dimensionless) is a shape parameter. Note that for $\delta_i = 0$, hydraulic restriction is at a minimum, while $\delta_i = 1$ corresponds to the classical linear shape (Brisson et al., 1998).

Water demand (maximum evapotranspiration [MET(t), mm]) was calculated on a daily basis using the commonly used Monteith's (Monteith & Moss, 1977) energy approach based on Beer's law,

$$MET(t) = PET(t) \times (1 - e^{-k \times LAI(t)}),$$

where PET(t) is the Penman potential evapotranspiration (Allen et al., 1998), k is the extinction coefficient that depends on canopy architecture (0.5 for forest), and LAI(t) is the Leaf Area Index. We used the same LAI seasonality curve across years and across species-size classes, as leaf phenology varies within a narrow range across species in this dry deciduous forest (Prasad & Hegde, 1986). The LAI curve was built from the literature (Prasad & Hegde, 1986),

corroborated by MODIS data (1999–2013) for the timing of leaf flush and senescence and varied as follows: from day 31 to 121 of the year LAI(t) (dimensionless) remained 0; from day 122 to 211 LAI(t) linearly increased from 0 to 7; then remained static at 7 until day 335; after which linearly decreased to 0 by day 31 of the next year.

The water demand is met on a daily basis from successively deeper compartments depending on the availability of water. Thus, for each species-size class total actual evapotranspiration (mm)

$$AET(t) = AET_1(t) + AET_2(t) + AET_3(t),$$

where $AET_i(t)$ is actual evapotranspiration from compartment C_i, and

$$AET_1(t) = minimum\left(M_1(t);\ MET(t)\ R_1\left(\frac{M_1(t)}{M_{1max}} \right)^{\delta_1} \right),$$

$$AET_2(t) = minimum\left(M_2(t);\ [MET(t) - AET_1(t)]\ R_2\left(\frac{M_2(t)}{M_{2max}} \right)^{\delta_2} \right),$$

$$AET_3(t) = minimum\left(M_3(t);\ [MET(t) - AET_1(t) - AET_2(t)]\ R_3\left(\frac{M_3(t)}{M_{3max}} \right)^{\delta_3} \right).$$

Successive uptake by depth is the most parsimonious way to model water uptake distribution by depth and such a simplification is commonly and successfully used in SVAT models (Brisson et al., 1998) and in Land Surface Models (Ducharne, Laval, & Polcher, 1998).

Water demand is supplied independently to each species-size class such that usage by one is not considered to deplete water available for others (Appendix S1.4).

For each species-size class, water-stress index over a period T is the proportion of water demand satisfied (range 0–1, dimensionless),

$$Stress\ Index_T = \frac{\sum_T AET(t)}{\sum_T MET(t)}.$$

When $\sum_T AET(t) = \sum_T MET(t)$, water demand is fully supplied, there is no stress and Stress Index$_T$ = 1, while when $\sum_T AET(t) = 0$, Stress Index$_T$ = 0.

2.3.3 | Water-stress model inversion based on observed growth rate to estimate water Uptake Depth Index

As in crop models, we assumed that stresses limit plants from achieving their growth potential, and used water-stress index (Stress Index$_T$) as a growth-reduction coefficient (Allen et al., 1998):

$$Observed\ growth_T = Stress\ Index_T \times Potential\ growth_T.$$

Thus at full satisfaction of water demand, Stress Index$_T$ = 1 and Observed growth$_T$ = Potential growth$_T$. Not ruling out other stresses on growth, we asked how much of observed variation in growth within species-size class is caused due to water stress. We

parameterized the water-stress model for each species-size class by selecting the top-10 best-fit parameter ensembles that would maximize the squared Pearson's correlation coefficient (r^2) between normalized time series of Observed growth$_{4-yearly}$ and the predicted Stress Index$_{4-yearly}$ from 1992 to 2012 (Figure S3). We used GLUE (Beven & Binley, 1992) to find best-fit parameter ensembles (R_1, R_2, R_3, δ_1, δ_2, δ_3, Figure S4) among 10,000 parameter ensembles generated by Latin Hypercube Sampling (McKay, Beckman, & Conover, 2000), after confirming that there was no issue of equifinality—see (Beven & Freer, 2001; Figure S5). Generalized likelihood uncertainty estimation identifies behavioural or acceptable set of parameter ensembles based on their likelihood surfaces (in this case, r^2) allowing for the possibility that multiple sets of parameter ensembles (even model structures, in general) can explain observed patterns in data (see Beven & Binley, 1992; Beven & Freer, 2001 for details on this methodology). Four out of 44 species-size classes that could not be parameterized well (best-fit $r^2 < .3$) were excluded from further analysis. Two understorey species which showed borderline equifinality issues in an exploratory analysis are not included in this manuscript. Uptake Depth Index (UDI$_T$) over a period T (e.g. annual, 20 years) was calculated for each species-size class as the mean of the compartment depth from which water is drawn, weighted by the proportion of the water drawn from that compartment (based on average of 10 best-fit model runs),

$$\text{UDI}_T = \frac{D_1 \sum_T \text{AET}_1(t) + D_2 \sum_T \text{AET}_2(t) + D_3 \sum_T \text{AET}_3(t)}{\sum_T \text{AET}(t)},$$

where $D_1 = 1$, $D_2 = 2$, and $D_3 = 3$ represents relative depths of compartment C_1, C_2 and C_3, respectively. A species' UDI$_T$ was defined as the average of UDI$_T$ for all size classes within species. UDI$_{mean}$ hereafter refers to UDI$_T$ over the study period of 20 years (1992–2012).

2.4 | Niche partitioning analyses

We tested whether species partitioned niches for below-ground water as a result of competition. For each species s, utilization p_{sj} of a below-ground compartment was calculated as the proportional use of compartment j over 1992–2012,

$$p_{sj} = \sum_{1992}^{2012} \frac{\text{AET}_j(t)}{\text{AET}(t)}.$$

Thus p_{sj}s of a species summed to 1. Species utilization of a resource could be greater due to preference for that resource (electivity) or greater availability of that resource. To calculate electivity e_{sj} of species s for compartment j we divided utilization p_{sj} by r_j, the relative availability of water in compartment j over 1992–2012. Thus,

$$e_{sj} = \frac{p_{sj}}{r_j},$$

where,

$$r_j = \sum_{1992}^{2012} \frac{M_j(t)}{M_1(t) + M_2(t) + M_3(t)}.$$

$r_1 = 0.23$, $r_2 = 0.33$, $r_3 = 0.44$ for compartments C_1, C_2 and C_3, respectively.

Niche overlap between species s and t were calculated using a pair-wise overlap statistic, Chzechanowski's Index (Feinsinger, Spears, & Poole, 1981; Gotelli & Graves, 1996):

$$O_{st} = O_{ts} = 1 - 0.5 \sum_{j=1}^{3} |e'_{sj} - e'_{tj}|$$

which ranges from 0 (no overlap) to 1 (complete overlap). A community-level overlap statistic was calculated as the mean of all species' pair-wise overlaps. We tested whether each of the observed pair-wise overlaps and the community-level niche overlap were smaller than their respective 5% simulation quantiles generated under the null model of no niche separation. Towards this, we generated 10,000 pseudo-communities by assuming that for each species utilization of any compartment is possible and the extent of utilization of one compartment is independent of other compartments (niche breadth is random; Gotelli & Graves, 1996; Silvertown, Dodd, Gowing, & Mountford, 1999). Each pseudo-community was generated by replacing utilization p_{sj} for every species-compartment combination by a random uniform variate (range 0–1). p_{sj}s within a species were then rescaled to sum to 1,

$$p'_{sj} = \frac{p_{sj}}{\sum_{i=1}^{3} p_{sj}}.$$

Electivities for all species-compartment combinations were then calculated. For each pseudo-community, Chzechanowski's Indices for all species pairs, as well as community-level mean overlap were calculated as described earlier to generate their null distributions. We also analysed how niche overlap between species pairs decreased with increasing distance from neighbour in vertical niche space (Gotelli & Graves, 1996; Inger & Colwell, 1977). Within the observed community, for a given species, its pair-wise niche overlap (Chzechanowski's Indices) with each of the $n - 1$ species was ordered with decreasing overlap and ranked 1 to $n - 1$ such that closer the rank to 1, greater the pair-wise overlap and closer the species neighbour in niche space. Such rank-overlap matrix was obtained for every species. For each rank then, a community-level rank-overlap matrix was calculated as a mean of overlaps across all species for that rank. We performed similar calculations for all 10,000 pseudo-communities to obtain a null distribution of the community-level rank-overlap matrix. At each rank, we tested whether the observed community-level niche overlap was smaller than the 5% simulation quantile. Results were similar when more conservative tests were used with pair-wise overlap statistic calculated as the geometric mean of utilization and electivity, $g_{sj} = \sqrt{e_{sj} p_{sj}}$, used to minimize bias towards large overlaps when certain resource states are very common (Gotelli & Graves, 1996; Winemiller & Pianka, 1990).

2.5 | Mortality analysis

To assess differential species mortality in response to extreme drought as a function of water uptake depth, we compared the difference in species percent mortality rate in year 2004 (following the extreme

drought of 2001–2003) from species pre-drought mortality rates (mean over the years 1997–1999) with species UDI_{2001}, a year for which divergence in species UDI_{annual} was largest (Figure 2b). For each species (Chitra-Tarak et al., 2017),

$$\%Mort_{drought} = \frac{\text{No. of tress dead}_{2004}}{\text{No. of trees present}_{2003}} \times 100,$$

$$\%Mort_{pre-drought} = 1/3\left(\sum_{yr=1997}^{yr=1999} \frac{\text{No. of trees dead}_{yr}}{\text{No. of trees present}_{yr-1}} \times 100\right).$$

Results were similar even when UDI_{mean} (that is, mean over 20 years) was used as a predictor (data not shown). Mortalities recorded as due to causes other than fire or large mammal herbivory alone were considered. Because tree death due to drought may play out over several years, we chose 2004 as the "treatment" year as mortality peaked in that year, but results were robust to use of cumulative mortality rates during and after the drought (cumulated over years 2001 through 2006). Mortality in other periods was low and stochastic (Figure S6). Therefore, although we used years 1997–1999, which were years of normal rainfall, to calculate background mortality rates, results were not sensitive to use of other periods. Results were similar with various tree size restrictions (above 1, 5, 10, or 20 cm DBH). We restricted analyses to six canopy species (accounting for 54% of trees ≥1 cm DBH and 79% ≥10 cm DBH) for which tree numbers in 2003 for the 50 ha MFDP were greater than 300. Species with sample sizes lower than 300 had high uncertainties in their $\%Mort_{drought}$ estimates based on bootstrapped CIs, as mortality rates due to causes other
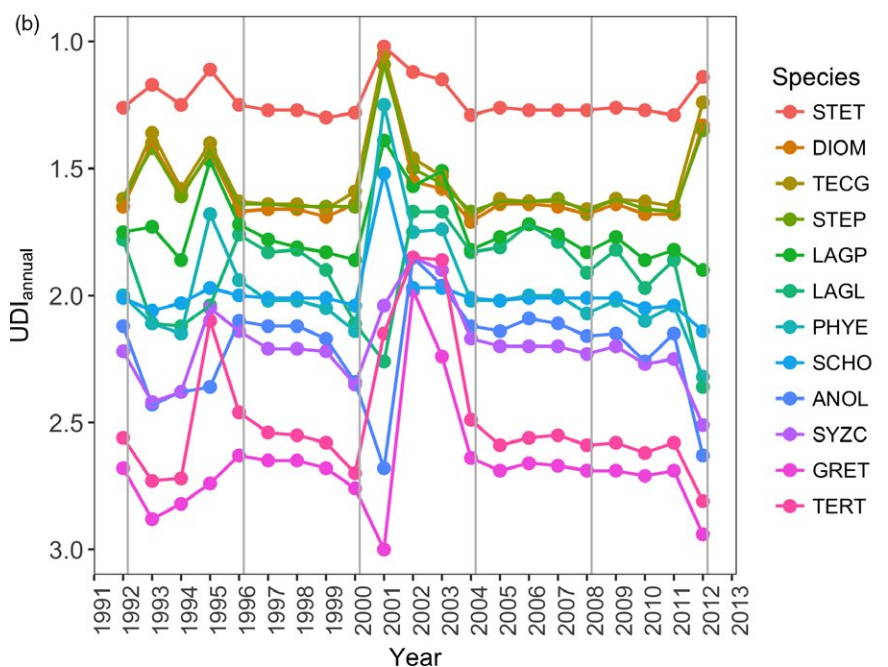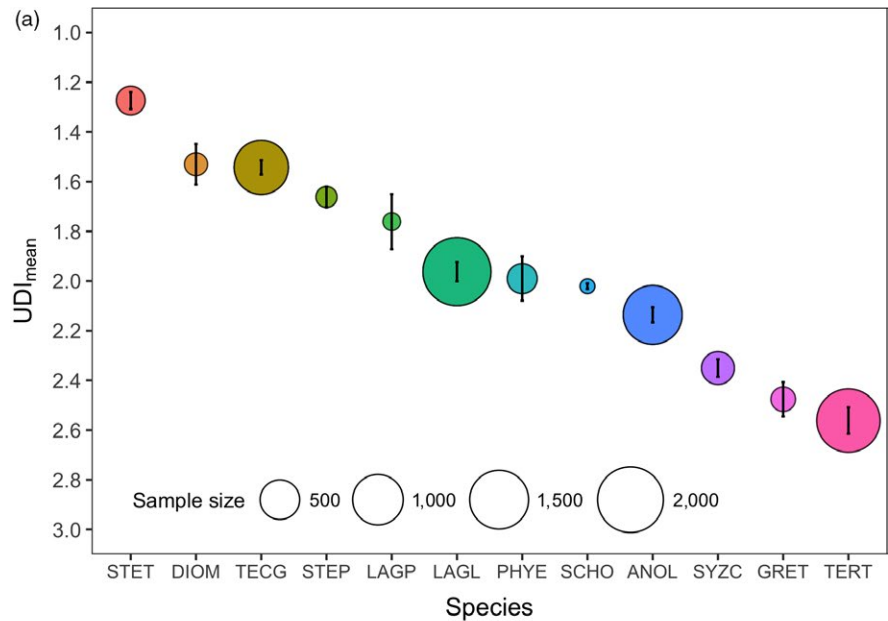
FIGURE 2 Estimated water Uptake Depth Index variation across species at MFDP. (a) Species UDI_{mean} ($M \pm SEM$ across size classes, $n = 5$ or 3, with 13–441 trees in each size class depending on species) is shown in circles, with symbol size proportional to the total sample size of trees for a given species. Colours vary by species. (b) Time series of species UDI_{annual} (mean across size classes, $n = 5$ or 3) from 1992 to 2012. Species codes represent: ANOL, *Anogeissus latifolia*; DIOM, *Diospyros montana*; GRET, *Grewia tiliifolia*; LAGL, *Lagerstroemia microcarpa*; LAGP, *Lagerstroemia parviflora*; PHYE, *Phyllanthus emblica*; SCHO, *Schleichera oleosa*; STEP, *Stereospermum personatum*; STET, *Stereospermum tetragonum*; SYZC, *Syzygium cumini*; TECG, *Tectona grandis*; TERT, *Terminalia crenulata* [Colour figure can be viewed at wileyonlinelibrary.com]

than fire or large mammal herbivory are very low in this forest (Suresh, Dattaraja, & Sukumar, 2010), making large sample sizes necessary for detecting a response.

See Appendix S1.5 for additional data and sensitivity analyses.

All analyses were performed using the R statistical platform, version 3.2.2 (R Core Team, 2015).

3 | RESULTS

3.1 | Vertical and temporal dynamics of water

In the study site, as hypothesized, COMFORT revealed the decoupling between the temporal dynamics of rainfall and water at depth, with high frequency variations at shallower depths reflecting daily or seasonal rainfall, and low frequency variations at deeper depths reflecting memory of decadal patterns in rainfall (Figure 1, Figure S2). At MFDP, for 1988–2012, correlations (Pearson's product-moment correlation coefficient, r) between mean annual water content of successively deeper compartments C_1, C_2 and C_3 and annual rainfall ($n = 25$) were 0.82, 0.76 and 0.34, with $p < .001$, <.001 and .16, respectively; and those for monthly rainfall ($n = 300$) were 0.58, 0.02 and 0.03 with $p < .001$, .7 and .6, respectively. Drying down and recharge times increased for deeper compartments. Vertical locations also correlated with different drought intensities. Especially in case of the exceptional succession of four drought years from 2000 to 2003, the deepest compartment [C_3] began depleting after 1 year (see 2001) and was eventually completely dry for 2 years (2002–2003). In contrast, the shallowest compartment [C_1] had seasonal availability of water throughout the drought, albeit less than normal. Droughts of less intensity (1993–1995; rainfall anomaly −20% to 25%) and/or duration (1989 rainfall anomaly −40%; 2012 rainfall anomaly −30%) depleted the deepest compartment only partially, and for shorter periods.

3.2 | Species differences in water uptake depths result in distinct growth patterns

There was high variability in growth patterns across species (Figure S1), which was successfully explained by the water-stress model (Figure S3), with species displaying contrasted hydraulic parameters Rs and δs (Figure S4) and distinct water uptake depths UDI$_{mean}$ (Figure 2a). Species differences in distribution of parameter R by depth may be thought to capture differences in rooting densities by depth, while species differences in δ, which regulates hydraulic restriction as compartments dry out may reflect differences in aboveground processes such as conductivity losses under negative water potential, or stomatal strategy. For each species, hydraulic parameter ensemble was well-constrained (absence of equifinality). In contrast to the model estimated Stress Index$_{4yearly}$, cumulative rain in the census interval was found to be a poor predictor of species growth, especially in cases of species that the model estimated to have deeper UDI$_{mean}$ (Figure S3). These results supported our second hypothesis that each species showed consistent growth response given its hydraulic/water uptake parameters and water availability by depth.

We found that UDI$_{mean}$ or relative water uptake by compartment did not systematically vary with stem size within species (Figure S7). Although larger trees have been reported to preferentially tap deeper water than smaller trees, the reverse has also been reported (Meinzer, Clearwater, & Goldstein, 2001). The lack of a systematic size-effect in this study is understandable given this fire-prone forest system, where regeneration is almost exclusively (>99%) via vegetative coppicing/ re-sprouting from burned stems with previously established root systems or from underground root-suckers (Mondal & Sukumar, 2015; Sukumar, Suresh, Dattaraj, John, & Joshi, 2004; Sukumar, Suresh, Dattaraja, Srinidhi, & Nath, 2005).

UDI$_{mean}$ did not show sensitivity to the shape of LAI seasonality curve that was varied across species (results not shown). Further, a test on a tree rings-based growth time series of *Tectona grandis* showed that UDI$_{mean}$ was similar whether we used the time series at annual (UDI$_{mean}$ = 1.5 ± 0.2) or 4-year scale (UDI$_{mean}$ = 1.3 ± 0.2) to parameterize the water-stress model (Appendix S1.5, Figure S8). In both the cases, variation in growth was explained well at lower (0%– 75%) values of Stress Index$_{annual}$, but not at higher values (>75%), most likely because at high stress (low value of Stress Index$_{annual}$), water may be the most limiting factor for growth, but when water availability is greater, growth is likely co-limited by other factors, such as light and nutrients. Leave-one-out cross-validation tests showed that the water-stress model was able to predict omitted values of the tree rings-based growth time series well (cross-validation NRMSE [normalized by range of growth rates]: 25% at annual scale and 5% at 4-year scale).

3.3 | Species hydrological niches evolve in vertical space and in time

The 20-year average of the Uptake Depth Index (UDI$_{mean}$, Figure 2a) revealed that most species used water below the soil compartment [C_1] (UDI$_{mean}$ > 1) and spanned a broad range of distinct values, demonstrating that the 12 common tree species partitioned hydrological niches in vertical space (Figure S9). The four co-dominant species (Appendix S1.1) expected to be in strong competition for the critical resource of water, displayed clearly distinct UDI$_{mean}$ values, supporting the hypothesis that competition drives hydrological niche separation. Mean community niche overlap based on electivity (0.52) was significantly lower than the null expectation ($p < .001$ for a one-tailed test at $\alpha = 5\%$; Figure S9a). Niche overlaps for half of the species pairs were significantly lower than their respective nulls (28 out of 66 species pairs with a one-tailed test at $\alpha = 5\%$). Analysis of how niche overlap between species pairs decreased with increasing distance from neighbour in vertical niche space revealed that although close neighbours (1–3) had highly overlapping niches, onwards to the fourth nearest neighbour observed overlaps were significantly lower than the overlaps predicted under the null model of no niche separation (Figure S9b; one-tailed tests at $\alpha = 5\%$).

The dynamics of annualized water Uptake Depth Index (UDI$_{annual}$) demonstrated the importance of temporal hydrological niches over decades. We were able to take advantage of an intensive drought that clearly fell in one growth census interval to investigate species-specific

temporal patterns of drought response. Species annualized relative water uptake from the three compartments remained stable except during this drought, where divergence in UDI_{annual} revealed differential species strategies (see Figure 2b, especially year 2001). After this in the exceptionally dry period of 2002–2003, most species UDI_{annual} values were lower (took water from shallower depths), as the deep vadose zone dried up.

3.4 | Greater water uptake depth results in greater mortality in the prolonged drought

Trees with deeper uptake depths suffered greater mortality during this drought than species whose relative water uptake depth was shallower (Figure 3). This was consistent with relative water availability by depth in the prolonged drought, with prolonged and intense water scarcity at deeper reservoirs compared to shallow reservoirs. We documented this for the six most abundant canopy species. This supports our hypothesis that species water uptake depth strategies result in differential mortality response to an extreme drought.

4 | DISCUSSION

4.1 | Evidence of spatio-temporal hydrological niches driving distinct species demography

In this study, we set out to illuminate very cryptic, but potentially critical processes that operate over decades, and that determine niche partitioning to vadose zone depths of over 20 m. Despite intraspecific growth variation and relatively coarse interval with which to detect growth patterns (4 years), a clear signal linked interspecific growth to the resource variation by depth provided by the hydrological model. This is substantial in part because individuals can show plasticity with respect to root investment both seasonally and over time (about 10% per year, Gill & Jackson, 2000) and yet we saw a clear pattern that species uptake water at very distinct depths.

Higher mortality of species with deeper uptake depth indices observed in the prolonged drought is consistent with our hydrological model, which projected prolonged and intense water scarcity at deeper reservoirs compared to shallow reservoirs owing to slow recharge dynamics (Figure 1). This suggests that trees specialized in deep-water uptake may, in fact, be poorly adapted to exceptional droughts with multi-decadal return times.

Our water-stress model further suggests that trade-offs between growth and mortality operate differently depending on species uptake depths (Figure 4). Species with deep UDI_{mean} are consistently close to their growth potential across most of the years, but show high stress and higher mortality when the deep-water resources become unavailable. Conversely, species with shallow UDI_{mean} are frequently far from their growth potential, but show less stress and no decline in survival during the long drought years, may be due to less disruptive dormancy in response to the rapid depletion and recharge dynamics of the shallow zone. These contrasting strategies have correlates across life-history theory. They follow the risk-averse (deep rooting), disturbance-tolerance (shallow rooting) spectrum.
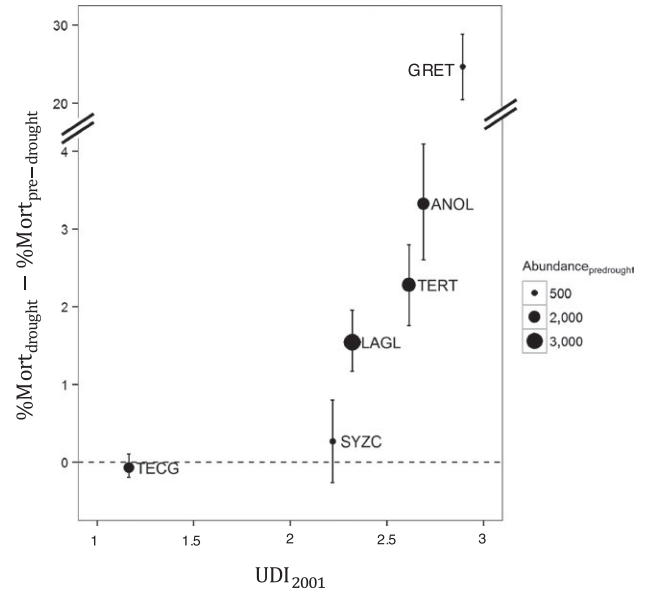

FIGURE 3 Greater UDI_{annual} results in higher mortality after an extreme drought. Difference in species drought (2004) and pre-drought (mean, 1997–1999) percent mortality rate, for trees greater than 5 cm DBH in the 50 ha MFDP are plotted against species UDI_{annual} for the moderate drought year 2001. Result is shown for UDI_{annual}, for species differences in UDI_{annual} were greatest in 2001, a year during the drought; however, observed trend was similar when UDI_{mean} was used as predictor. For each species s,

$$\%Mort_{drought} = \frac{\text{No. of trees dead}_{2004}}{\text{No. of trees present}_{2003}} \times 100 \text{ and}$$

$$\%Mort_{pre-drought} = 1/3 \left(\sum_{yr=1997}^{yr=1999} \frac{\text{No. of trees dead}_{yr}}{\text{No. of trees present}_{yr-1}} \times 100 \right). \text{ Error}$$

bars are 95% bootstrapped CI for $\%Mort_{drought}$. Symbol size is proportional to species $Abundance_{pre-drought}$.

In the same 50 ha MFDP, Pulla, Suresh, Dattaraja, and Sukumar (2017) found no niche differences among three of the top-four co-dominant species (Appendix S1.1) when tested using common axes of soil nutrients, topography and annual precipitation. That the present study could reveal niche differences in these species along vertical axis of hydrological niche segregation highlights the latter's value in explaining species coexistence in diverse forest systems.

4.2 | A call to study the drought species experience

We propose that species water uptake depths should be explored within a broader, more comprehensive approach to species-specific drought response. If there is an apparent lack of a link between drought events and mortality, this should not be taken as evidence that a species is "drought-tolerant" unless it is demonstrated that that species actually experienced reduced water availability. That is, the species-specific "experienced" drought matters for demography and not meteorological "drought."

Thus, we believe that the manner in which drought status is assessed and assigned to a species can be greatly improved by combining hydro-logical models of water movement through forests with the expansive
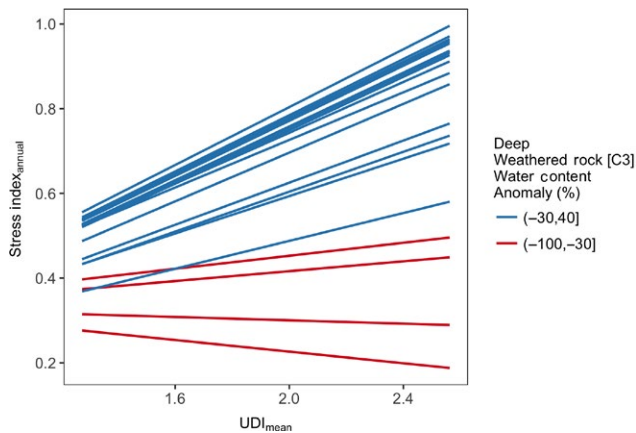
FIGURE 4 Contrasts in experienced water stress depending on species UDI_{mean} and drought intensity of the year. To summarize the general trend across species in temporal behaviour as captured by the inversion of the water-stress model, regressions between the two model estimates—species UDI_{mean} & Stress $Index_{annual}$ (water supply-to-demand ratio)—are computed using a Linear Mixed Effects model, with a random intercept and slope for grouping variable year ($n = 280$; years (grouping factor) = 20). For each year from 1992 to 2012, species Stress $Index_{annual}$ predicted from this LME model is presented as a function of species UDI_{mean}, colour coded by percent Deep Weathered Rock zone [C_3] water content anomaly for that year. For clarity, only regression lines are shown and not individual points [Colour figure can be viewed at wileyonlinelibrary.com]

data emerging from global monitoring sites on tree growth and mortality. Our water-stress model that estimates dynamics of realized plant water uptake depths vis-à-vis water availability facilitates this advance.

4.3 | The challenge of identifying below-ground community processes

Direct observations of the root activity of communities over large time-scales are essentially impossible with standard methods used to assess rooting systems (e.g. pits, soil cores, DNA barcoding or isotopic tracers, Maeght, Rewald, & Pierret, 2013; McDonnell, 2014; Meinzer et al., 2001). These methods are either destructive, unrepeatable over intensive temporal or spatial domains, or they may identify the presence, but not the activity of roots.

Inverse modelling of forest water stress, based on globally available community-level observations (e.g. AET from remote sensing) and use of phenomenological and conceptual (lumped) model parameters, are now common ways of estimating maximum rooting depth at the community level (Fan, Miguez-Macho, Jobbágy, Jackson, & Otero-Casal, 2017; Gao et al., 2014). We have expanded this approach to species/size class by using growth data from long-term surveys. Our approach was able to use data at larger spatial scales (watershed and stand) to infer the water trees have access to over decades, and the consequences of having that access. Our method is able to rank the species according to their relative depth of water uptake, but there is a large uncertainty about their absolute uptake depth considering the possible range of the vadose zone thickness in the present study

(15–40 m, see Appendix S1.6). The scale of community-wide water access over decades addressed in this study may not necessarily gain from soil moisture readings near the surface, nor from snap-shots of leaf water potentials from several trees (due to mismatch between the scales of model components and observation).

4.4 | Significance, generality and future directions

To our knowledge, this is the first time a mechanistic link between hydrological niche separation and tree demography has been documented for a diverse tropical forest community. We have shown that, for the long-lived forest trees, hydrological niche dynamics play out over decades through interaction with a deep vadose zone. The depth of this ecosystem, underestimated by virtually all models dealing with vegetation–climate interactions, lends the eco-hydrological system a long memory for past climate patterns and cyclical rainfall variation with seasonal, supra-annual, decadal (like ENSO or IOD) and perhaps even longer return times. We expect such mechanisms to be globally significant, as differential water dynamics by depth is commonly observed, and decoupled dynamics of precipitation and water availability is expected to be a general phenomenon, although scales may vary. Although it is reported more from agricultural sites (Entin et al., 2000; Turkeltaub, Dahan, & Kurtzman, 2014), in forested catchments where uptake can be far deep, differences in dynamics by depth is expected to be even greater. Deep-rootedness is increasingly found to be ubiquitous across seasonally dry, semi-arid to humid regions under vegetation types as varied as savanna, thorn-scrub, seasonally deciduous and evergreen forests (Ohnuki et al., 2008; Schenk & Jackson, 2002; Schwinning, 2010). These mechanisms might have played a significant role in drought-driven changes in composition and function that have been demonstrated in Amazonian (Doughty et al., 2015), African (Phillips et al., 2010), and south-east Asian (Van Nieuwstadt & Sheil, 2005) tropical forests and savannas (Fensham, Fairfax, & Ward, 2009), as well as in temperate and boreal forests (Ma et al., 2012). Exploring these mechanisms has become even more important as climate is changing in mean state as well as in variability, with projected increase in drought frequency and intensity (IPCC, 2013) that can change the specific frequency in patterns of water availability that each tree species is adapted to. As technologies advance, we would hope that methods will become available that would simultaneously monitor soil water contents throughout the vadose zone as well as stand-wide measurements of leaf water potentials over the long term. Yet these technologies are not available. We call for a gathering of existing, long-term forest demography and hydrological datasets across the globe to be synthesized in the proposed analytical framework to better understand species coexistence across forest types and improve mechanistic predictions of productivity and compositional change under future drought.

AUTHORS' CONTRIBUTIONS

R.S. conceived, established and coordinated the Mudumalai FDP programme; H.S.D. and H.S.S. coordinated and collected field data; L.R. conceived and established; L.R., M.S.M.K. and J.R. coordinated Mulehole hydrological monitoring programme; L.R. and J.R. collected field data; R.C.T. and L.R. conceived the idea and designed the study, and carried out data analyses and interpretations; R.C.T., L.R., S.M.M. and R.S. wrote the paper. All authors read and approved the final manuscript. The authors declare that they have no conflicts of interest.

DATA ACCESSIBILITY

Data available from the Dryad Digital Repository: https://doi.org/10.5061/dryad.nm3d3 (Chitra-Tarak et al., 2017). Hydrological and meteorological data for Mulehole catchment are open access and available to download from the ORE-BVET project site: http://bvet.obs-mip.fr/en/Data-access.

ORCID

Rutuja Chitra-Tarak [iD] http://orcid.org/0000-0001-9714-7524

Laurent Ruiz [iD] http://orcid.org/0000-0001-5043-282X

Handanakere S. Dattaraja [iD] http://orcid.org/0000-0003-1140-5700

M. S. Mohan Kumar [iD] http://orcid.org/0000-0003-0478-7237

Jean Riotte [iD] http://orcid.org/0000-0002-5563-1913

Hebbalalu S. Suresh [iD] http://orcid.org/0000-0003-4753-3595

Sean M. McMahon [iD] http://orcid.org/0000-0001-8302-6908

Raman Sukumar [iD] http://orcid.org/0000-0001-9077-7822

REFERENCES

Allen, C. D., Breshears, D. D., & McDowell, N. G. (2015). On underestimation of global vulnerability to tree mortality and forest die-off from hotter drought in the Anthropocene. *Ecosphere*, 6, 1–55. https://doi.org/10.1890/ES15-00203.1

Allen, C. D., Macalady, A. K., Chenchouni, H., Bachelet, D., McDowell, N., Vennetier, M., ... Cobb, N. (2010). A global overview of drought and heat-induced tree mortality reveals emerging climate change risks for forests. *Forest Ecology and Management*, 259, 660–684. https://doi.org/10.1016/j.foreco.2009.09.001

Allen, R. G., Pereira, L. S., Raes, D., & Smith, M. (1998). *Crop evapotranspiration – Guidelines for computing crop water requirements – FAO Irrigation and drainage paper 56*. Rome, Italy: FAO - Food and Agriculture Organization of the United Nations.

Anderegg, L. D. L., Anderegg, W. R. L., & Berry, J. A. (2013). Not all droughts are created equal: Translating meteorological drought into woody plant mortality. *Tree Physiology*, 33, 672–683. https://doi.org/10.1093/treephys/tpt044

Anderegg, W. R. L., Kane, J. M., & Anderegg, L. D. L. (2013). Consequences of widespread tree mortality triggered by drought and temperature stress. *Nature Climate Change*, 3, 30–36. https://doi.org/10.1038/nclimate1635

Beven, K., & Binley, A. (1992). The future of distributed models: Model calibration and uncertainty prediction. *Hydrological Processes*, 6, 279–298. https://doi.org/10.1002/hyp.3360060305

Beven, K., & Freer, J. (2001). Equifinality, data assimilation, and uncertainty estimation in mechanistic modelling of complex environmental systems using the GLUE methodology. *Journal of Hydrology*, 249, 11–29. https://doi.org/10.1016/S0022-1694(01)00421-8

Braun, J.-J., Descloitres, M., Riotte, J., Fleury, S., Barbiéro, L., Boeglin, J.-L., ... Dupré, B. (2009). Regolith mass balance inferred from combined mineralogical, geochemical and geophysical studies: Mule Hole gneissic watershed, South India. *Geochimica et Cosmochimica Acta*, 73, 935–961. https://doi.org/10.1016/j.gca.2008.11.013

Brisson, N., Mary, B., Ripoche, D., Jeuffroy, M. H., Ruget, F., Nicoullaud, B., ... Delécolle, R. (1998). STICS: A generic model for the simulation of crops and their water and nitrogen balances. I. Theory and parameterization applied to wheat and corn. *Agronomie*, 18, 311–346. https://doi.org/10.1051/agro:19980501

Chitra-Tarak, R., Ruiz, L., Dattaraja, H. S., Mohan Kumar, M. S., Suresh, H. S., Riotte, J., ... Sukumar, R. (2017). Data from: The roots of the drought: Hydrology and water uptake strategies mediate forest-wide demographic response to precipitation. *Dryad Digital Repository*, https://doi.org/10.5061/dryad.nm3d3

Choat, B., Jansen, S., Brodribb, T. J., Cochard, H., Delzon, S., Bhaskar, R., ... Zanne, A. E. (2012). Global convergence in the vulnerability of forests to drought. *Nature*, 491, 752–755.

Condit, R., Lao, S., Singh, A., Esufali, S., & Dolins, S. (2014). Data and database standards for permanent forest plots in a global network. *Forest Ecology and Management*, 316, 21–31. https://doi.org/10.1016/j.foreco.2013.09.011

Couvreur, V., Vanderborght, J., & Javaux, M. (2012). A simple three-dimensional macroscopic root water uptake model based on the hydraulic architecture approach. *Hydrology and Earth System Sciences*, 16, 2957–2971. https://doi.org/10.5194/hess-16-2957-2012

Cramer, W., Bondeau, A., Woodward, F. I., Prentice, I. C., Betts, R. A., Brovkin, V., ... Young-Molling, C. (2001). Global response of terrestrial ecosystem structure and function to CO_2 and climate change: Results from six dynamic global vegetation models. *Global Change Biology*, 7, 357–373. https://doi.org/10.1046/j.1365-2486.2001.00383.x

Dattaraja, H. S., Mondal, N., Pulla, S., Suresh, H. S., Bharnnaiah, C. M., & Sukumar, R. (2013). *Spatial interpolation of rainfall for Mudumalai wildlife sanctuary and tiger reserve, Tamil Nadu, India*. CES Technical Report. Bangalore, India: Centre for Ecological Sciences, Indian Institute of

Science. Retrieved from http://wgbis.ces.iisc.ernet.in/biodiversity/pubs/ces_tr/TR130/TR130.pdf

Descloitres, M., Ruiz, L., Sekhar, M., Legchenko, A., Braun, J.-J., Kumar, M., & Subramanian, S. (2008). Characterization of seasonal local recharge using electrical resistivity tomography and magnetic resonance sounding. *Hydrological Processes*, *22*, 384–394. https://doi.org/10.1002/hyp.6608

Doughty, C. E., Metcalfe, D. B., Girardin, C. A. J., Amézquita, F. F., Cabrera, D. G., Huasco, W. H., … Malhi, Y. (2015). Drought impact on forest carbon dynamics and fluxes in Amazonia. *Nature*, *519*, 78–82. https://doi.org/10.1038/nature14213

Ducharne, A., Laval, K., & Polcher, J. (1998). Sensitivity of the hydrological cycle to the parametrization of soil hydrology in a GCM. *Climate Dynamics*, *14*, 307–327. https://doi.org/10.1007/s003820050226

Entin, J. K., Robock, A., Vinnikov, K. Y., Hollinger, S. E., Liu, S., & Namkhai, A. (2000). Temporal and spatial scales of observed soil moisture variations in the extratropics. *Journal of Geophysical Research: Atmospheres*, *105*, 11865–11877. https://doi.org/10.1029/2000JD900051

Fan, Y., Miguez-Macho, G., Jobbágy, E. G., Jackson, R. B., & Otero-Casal, C. (2017). Hydrologic regulation of plant rooting depth. *Proceedings of the National Academy of Sciences of the United States of America*, *114*, 10572–10577. https://doi.org/10.1073/pnas.1712381114

Feinsinger, P., Spears, E. E., & Poole, R. W. (1981). A simple measure of niche breadth. *Ecology*, *62*, 27–32. https://doi.org/10.2307/1936664

Fensham, R. J., Fairfax, R. J., & Ward, D. P. (2009). Drought-induced tree death in savanna. *Global Change Biology*, *15*, 380–387. https://doi.org/10.1111/j.1365-2486.2008.01718.x

Friend, A. D., Lucht, W., Rademacher, T. T., Keribin, R., Betts, R., Cadule, P., … Woodward, F. I. (2014). Carbon residence time dominates uncertainty in terrestrial vegetation responses to future climate and atmospheric CO_2. *Proceedings of the National Academy of Sciences of the United States of America*, *111*, 3280–3285. https://doi.org/10.1073/pnas.1222477110

Gao, H., Hrachowitz, M., Schymanski, S. J., Fenicia, F., Sriwongsitanon, N., & Savenije, H. H. G. (2014). Climate controls how ecosystems size the root zone storage capacity at catchment scale. *Geophysical Research Letters*, *41*, 7916–7923. https://doi.org/10.1002/2014GL061668

Gill, R. A., & Jackson, R. B. (2000). Global patterns of root turnover for terrestrial ecosystems. *New Phytologist*, *147*, 13–31. https://doi.org/10.1046/j.1469-8137.2000.00681.x

Gotelli, N. J., & Graves, G. R. (1996). *Null models in ecology*. Washington, DC: Smithsonian Institution Press.

Ichii, K., Hashimoto, H., White, M. A., Potter, C., Hutyra, L. R., Huete, A. R., … Nemani, R. R. (2007). Constraining rooting depths in tropical rainforests using satellite data and ecosystem modeling for accurate simulation of gross primary production seasonality. *Global Change Biology*, *13*, 67–77. https://doi.org/10.1111/j.1365-2486.2006.01277.x

Inger, R. F., & Colwell, R. K. (1977). Organization of contiguous communities of amphibians and reptiles in Thailand. *Ecological Monographs*, *47*, 229–253. https://doi.org/10.2307/1942516

IPCC. (2013). *Climate change 2013: The physical science basis*. In T. F. Stocker, D. Qin, G.-K. Plattner, M. Tignor, S. K. Allen, J. Boschung, A. Nauels, Y. Xia, V. Bex, & P. M. Midgley (Eds.). Cambridge, UK: Cambridge University Press. Retrieved from http://www.climatechange2013.org

Ma, Z., Peng, C., Zhu, Q., Chen, H., Yu, G., Li, W., … Zhang, W. (2012). Regional drought-induced reduction in the biomass carbon sink of Canada's boreal forests. *Proceedings of the National Academy of Sciences of the United States of America*, *109*, 2423–2427. https://doi.org/10.1073/pnas.1111576109

Maeght, J.-L., Rewald, B., & Pierret, A. (2013). How to study deep roots – And why it matters. *Frontiers in Plant Science*, *4*, 299. https://doi.org/10.3389/fpls.2013.00299

McDonnell, J. J. (2014). The two water worlds hypothesis: Ecohydrological separation of water between streams and trees? *Wiley Interdisciplinary Reviews: Water*, *1*, 323–329. https://doi.org/10.1002/wat2.1027

McDowell, N., Pockman, W. T., Allen, C. D., Breshears, D. D., Cobb, N., Kolb, T., … Yepez, E. A. (2008). Mechanisms of plant survival and mortality during drought: Why do some plants survive while others succumb to drought? *New Phytologist*, *178*, 719–739. https://doi.org/10.1111/j.1469-8137.2008.02436.x

McKay, M. D., Beckman, R. J., & Conover, W. J. (2000). A comparison of three methods for selecting values of input variables in the analysis of output from a computer code. *Technometrics*, *42*, 55–61. https://doi.org/10.1080/00401706.2000.10485979

Meinzer, F. C., Clearwater, M. J., & Goldstein, G. (2001). Water transport in trees: Current perspectives, new insights and some controversies. *Environmental and Experimental Botany*, *45*, 239–262. https://doi.org/10.1016/S0098-8472(01)00074-0

Meir, P., Mencuccini, M., & Dewar, R. C. (2015). Drought-related tree mortality: Addressing the gaps in understanding and prediction. *New Phytologist*, *207*, 28–33. https://doi.org/10.1111/nph.13382

Mondal, N., & Sukumar, R. (2015). Regeneration of juvenile woody plants after fire in a seasonally dry tropical forest of Southern India. *Biotropica*, *47*, 330–338. https://doi.org/10.1111/btp.12219

Monteith, J. L., & Moss, C. J. (1977). Climate and the efficiency of crop production in Britain [and discussion]. *Philosophical Transactions of the Royal Society of London B: Biological Sciences*, *281*, 277–294. https://doi.org/10.1098/rstb.1977.0140

Ohnuki, Y., Shimizu, A., Chann, S., Toriyama, J., Kimhean, C., & Araki, M. (2008). Seasonal change in thick regolith hardness and water content in a dry evergreen forest in Kampong Thom Province, Cambodia. *Geoderma*, *146*, 94–101. https://doi.org/10.1016/j.geoderma.2008.05.016

Phillips, O. L., van der Heijden, G., Lewis, S. L., López-González, G., Aragão, L. E. O. C., Lloyd, J., … Vilanova, E. (2010). Drought–mortality relationships for tropical forests. *New Phytologist*, *187*, 631–646. https://doi.org/10.1111/j.1469-8137.2010.03359.x

Prasad, S. N., & Hegde, M. (1986). Phenology and seasonality in the tropical deciduous forest of Bandipur, South India. *Proceedings of the Indian Academy of Sciences: Plant Sciences*, *96*, 121–133.

Pulla, S., Riotte, J., Suresh, H. S., Dattaraja, H. S., & Sukumar, R. (2016). Controls of soil spatial variability in a dry tropical forest. *PLoS ONE*, *11*, e0153212. https://doi.org/10.1371/journal.pone.0153212

Pulla, S., Suresh, H. S., Dattaraja, H. S., & Sukumar, R. (2017). Multidimensional tree niches in a tropical dry forest. *Ecology*, *98*, 1334–1348. https://doi.org/10.1002/ecy.1788

R Core Team. (2015). *R: A language and environment for statistical computing*. Vienna, Austria: R Foundation for Statistical Computing.

Riotte, J., Maréchal, J. C., Audry, S., Kumar, C., Bedimo, J. P., Ruiz, L., … Braun, J. J. (2014). Vegetation impact on stream chemical fluxes: Mule Hole watershed (South India). *Geochimica et Cosmochimica Acta*, *145*, 116–138. https://doi.org/10.1016/j.gca.2014.09.015

Rodriguez-Iturbe, I. (2000). Ecohydrology: A hydrologic perspective of climate-soil-vegetation dynamies. *Water Resources Research*, *36*, 3–9. https://doi.org/10.1029/1999WR900210

Rodriguez-Iturbe, I., Porporato, A., Laio, F., & Ridolfi, L. (2001). Intensive or extensive use of soil moisture: Plant strategies to cope with stochastic water availability. *Geophysical Research Letters*, *28*, 4495–4497. https://doi.org/10.1029/2001GL012905

Ruiz, L., Varma, M. R., Kumar, M. M., Sekhar, M., Maréchal, J.-C., Descloitres, M., … Braun, J.-J. (2010). Water balance modelling in a tropical watershed under deciduous forest (Mule Hole, India): Regolith matric storage buffers the groundwater recharge process. *Journal of Hydrology*, *380*, 460–472. https://doi.org/10.1016/j.jhydrol.2009.11.020

Schenk, H. J., & Jackson, R. B. (2002). Rooting depths, lateral root spreads and below-ground/above-ground allometries of plants in water-limited ecosystems. *Journal of Ecology*, *90*, 480–494. https://doi.org/10.1046/j.1365-2745.2002.00682.x

Schwinning, S. (2010). The ecohydrology of roots in rocks. *Ecohydrology*, *3*, 238–245. https://doi.org/10.1002/eco.134

Schwinning, S., & Kelly, C. K. (2013). Plant competition, temporal niches and implications for productivity and adaptability to climate change in water-limited environments. *Functional Ecology*, *27*, 886–897. https://doi.org/10.1111/1365-2435.12115

Silvertown, J., Araya, Y., & Gowing, D. (2015). Hydrological niches in terrestrial plant communities: A review. *Journal of Ecology*, *103*, 93–108. https://doi.org/10.1111/1365-2745.12332

Silvertown, J., Dodd, M. E., Gowing, D. J. G., & Mountford, J. O. (1999). Hydrologically defined niches reveal a basis for species richness in plant communities. *Nature*, *400*, 61–63. https://doi.org/10.1038/21877

Sukumar, R., Dattaraja, H. S., Suresh, H. S., Radhakrishnan, J., Vasudeva, R., Nirmala, S., & Joshi, N. V. (1992). Long-term monitoring of vegetation in a tropical deciduous forest in Mudumalai, southern India. *Current Science*, *62*, 608–616.

Sukumar, R., Suresh, H. S., Dattaraj, H. S., John, R., & Joshi, N. V. (2004). Mudumalai forest dynamics plot, India. In E. C. Losos, & E. G. Leigh (Eds.), *Tropical forest diversity and dynamics: Findings from a large-scale plot network* (pp. 551–563). Chicago, IL: University of Chicago Press.

Sukumar, R., Suresh, H. S., Dattaraja, H. S., Srinidhi, S., & Nath, C. (2005). The dynamics of a tropical dry forest in India: Climate, fire, elephants and the evolution of life-history strategies. In D. Burslem, M. Pinard, & S. Hartley (Eds.), *Biotic interactions in the tropics: Their role in the maintenance of species diversity* (pp. 510–529). Cambridge, UK: Cambridge University Press. https://doi.org/10.1017/CBO9780511541971.022

Suresh, H. S., Dattaraja, H. S., & Sukumar, R. (2010). Relationship between annual rainfall and tree mortality in a tropical dry forest: Results of a 19-year study at Mudumalai, southern India. *Forest Ecology and Management*, *259*, 762–769. https://doi.org/10.1016/j.foreco.2009.09.025

Turkeltaub, T., Dahan, O., & Kurtzman, D. (2014). Investigation of groundwater recharge under agricultural fields using transient deep vadose zone data. *Vadose Zone Journal*, *13*. https://doi.org/10.2136/vzj2013.10.0176

Van Nieuwstadt, M. G., & Sheil, D. (2005). Drought, fire and tree survival in a Borneo rain forest, East Kalimantan, Indonesia. *Journal of Ecology*, *93*, 191–201. https://doi.org/10.1111/j.1365-2745.2004.00954.x

Winemiller, K. O., & Pianka, E. R. (1990). Organization in natural assemblages of desert lizards and tropical fishes. *Ecological Monographs*, *60*, 27–55. https://doi.org/10.2307/1943025

SUPPORTING INFORMATION

Additional Supporting Information may be found online in the supporting information tab for this article.

How to cite this article: Chitra-Tarak R, Ruiz L, Dattaraja HS, et al. The roots of the drought: Hydrology and water uptake strategies mediate forest-wide demographic response to precipitation. *J Ecol.* 2018;106:1495–1507. https://doi.org/10.1111/1365-2745.12925